

## CASSCF Study of the Ground State and Lowest Lying 3s Rydberg States of ABCO

R. Disselkamp,<sup>†</sup> Q.-Y. Shang,<sup>‡</sup> and E. R. Bernstein\*

Department of Chemistry, Colorado State University, Fort Collins, Colorado 80523

Received: April 27, 1994; In Final Form: August 12, 1994<sup>®</sup>

An *ab initio* CASSCF study of the ground and first two excited 3s Rydberg states ( $A_1$ , E) of azabicyclo[2.2.2]octane (ABCO) is presented. The calculations support a previous assignment of the lowest energy transition of ABCO as  $2A_1 \leftarrow 1A_1$ . The excited Rydberg state molecular orbital  $2A_1$  is composed of 2p nitrogen, 3s nitrogen, and 3s carbon orbitals. An examination of the HOMO and LUMO natural orbitals for this state suggests that the atomic 3s carbon orbitals located on the carbon atoms bonded to the tertiary nitrogen atom contribute roughly 80% to each orbital. In fact, on the basis of these calculations, a more accurate description of this Rydberg transition is as a two-electron excitation from  $S_0[2p_z(N)]^2$  to a partially delocalized  $R_1[3s(C)3s(N)]^2$ . The transition  $2A_1 \leftarrow 1A_1$  is found experimentally at  $39\,080\text{ cm}^{-1}$  and is calculated to appear at  $36\,067\text{ cm}^{-1}$ . An extended basis set calculation employing [3s plus  $3p_{x,y,z}(N)$ ] orbitals does not alter these conclusions significantly. The second excited Rydberg state (of E symmetry) is calculated to lie ca.  $4000\text{ cm}^{-1}$  above the first. This state is calculated at the 3s active space level to be composed of a  $2p_z$  nitrogen orbital (HOMO) and carbon atomic 3s orbitals located on the carbon atoms bonded to the nitrogen atom (LUMO). Employing a [3s plus  $3p(N)$ ] active space again has only a small effect on the orbital composition of the excited E Rydberg state. On the basis of the energy separation between the  $2A_1$  and E Rydberg states, one can assign the second observed Rydberg transition to the  $E \leftarrow 1A_1$  excitation. Geometry-optimized structures show that the C-N-C apex angle increases upon electronic excitation  $R_2, R_1 \leftarrow S_0$ , supporting a previous assignment of cage compression vibrational modes in the vibronic activity of these transitions. The effect of Rydberg state excitation is analyzed in terms of charge redistribution in the ABCO molecule.

## I. Introduction

The Rydberg states of ammonia are generally thought to be atomic-like with regard to the excited states of the nitrogen atom (3s, 3p, 3d, etc.).<sup>1</sup> Alkyl-substituted amines can have Rydberg states that are either atomic nitrogen-like or have contributions from all or some of the carbon atomic Rydberg orbitals. In this study we explore the low-lying excited Rydberg states of ABCO (azabicyclo[2.2.2]octane, Figure 1) by *ab initio* CASSCF methods, to elucidate the orbital composition and nature of the Rydberg states of one such alkyl amine. Molecular Rydberg states are typically interpreted on the basis of quantum defect values (an atom-based picture), the validity of which for ABCO will be explored in this report. The possibility that more than a single 3s state is observed in these systems has not been explored. Such an assignment could not be unambiguously made based on quantum defect values. Since ABCO has  $C_{3v}$  point group symmetry (Figure 1) and both one- and two-photon transitions are allowed to both  $A_1$  and E excited vibronic states, the nature of these states cannot be uniquely decided by spectroscopic evidence alone.<sup>2</sup>

The first study of the electronic spectra of ABCO was performed on a room temperature sample;<sup>3,4</sup> three electronic states were identified with extensive vibrational structure assigned to  $\nu_1(S_0, 1100\text{ cm}^{-1})$ ,  $\nu_2(S_0, 290\text{ cm}^{-1})$ , and  $\nu_3(S_0, 625\text{ cm}^{-1})$  modes. The most prevalent progression forming mode was assigned as  $\nu_3$ , the cage compression mode. The origins of these transitions lie at  $39\,080\text{ cm}^{-1}$  ( $f \sim 0.003$ ),  $43\,750\text{ cm}^{-1}$  ( $f \sim 0.06$ ), and  $44\,700\text{ cm}^{-1}$  ( $f \sim 0.06$ ). These transitions were tentatively assigned<sup>3,4</sup> as  $(2p\sigma^*) \leftarrow (2p)^2$  (valence),  $(2p3p_z)$

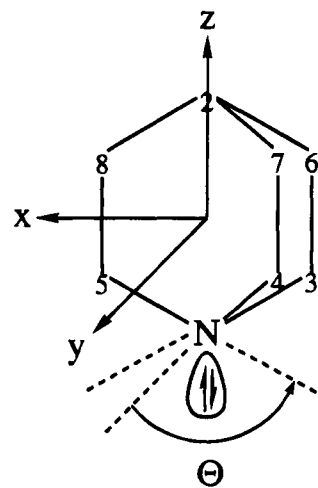


**Figure 1.** Coordinate system used in the calculation of 1-azabicyclo[2.2.2]octane (ABCO,  $C_{3v}$  symmetry). The (C-N-C) angle  $\Theta$  corresponds to the angle between nitrogen-carbon bonds. Three such angles can be identified, and all three are equal. The numbering system for the atoms is also given (N is atom 1).

$\leftarrow (2p)^2$  (Rydberg), and  $(2p4p_z)^2 \leftarrow (2p)^2$  (Rydberg), respectively. The second and third transitions were assigned on the basis of a calculated quantum defect of  $\delta \sim 0.5$ , indicative of a p-type Rydberg series.

The first multiphoton ionization study of ABCO was performed by Parker and Avouris.<sup>2</sup> Their two-photon room temperature  $S_2, S_1 \leftarrow S_0$  spectra confirm the vibrational assignments of refs 3 and 4; however, they reassigned the electronic transitions and the excited state electronic configurations. The  $S_1$  state was reassigned as a  $(2p3s)$  Rydberg state of  $A_1$  symmetry on the basis of two observations: (1) a quantum

<sup>†</sup> Current address: CIRES, University of Colorado, Boulder, CO 80309.

<sup>‡</sup> Current address: Applied Materials, Santa Clara, CA 95054.

<sup>®</sup> Abstract published in *Advance ACS Abstracts*, May 1, 1995.

defect of  $\delta \sim 0.8$  and (2) the transitions could be observed by an MPI technique (that is, the excited state lifetimes are long). The second excited electronic state was reassigned to a N atom localized  $3p_{x,y}$  Rydberg state of E symmetry on the basis of  $\delta \sim 0.5$  and analogies to the electronic assignments made for the diazabicyclooctane (DABCO) and ammonia systems.<sup>2,5</sup>

Recent studies of ABCO excited electronic states have employed two-photon spectroscopy, supersonic jet cooling, and mass detection techniques for both the bare molecule and various clusters.<sup>6,7</sup> Solvent enhanced intersystem crossing and Rydberg state to solvent energy and electron transfer have been demonstrated in the clusters.<sup>7</sup>

*Ab initio* quantum chemistry studies of ABCO have also appeared,<sup>8</sup> the series of substituted amines  $\text{NH}_3$ ,  $\text{N}(\text{CH}_3)_3$ , ABCO, and DABCO were systematically investigated employing a minimal STO-3G basis set augmented with Rydberg s- and p-type functions. Ground and excited state energies were obtained using a direct configuration interaction (CI) algorithm which performed double excitations from the highest occupied orbital of the ground state (i.e., nitrogen 2p lone-pair orbital) into the complete virtual space. These calculations support the above assignments; this study did not consider the possibility of multiple 3s Rydberg states in the same energy region, however.

The discussion of our results begins with an outline of the computational procedures employed. Results are then presented and discussed in two parts. First, electronic state assignments are made and the effect of Rydberg excitation on molecular geometry is explored. Second, natural orbital results are interpreted to give insight into the electronic distribution in the Rydberg states. Two basis sets are employed for this latter determination: one using carbon and nitrogen 3s atomic orbitals and one using the same 3s atomic orbitals augmented by nitrogen 3p orbitals.

## II. Computational Details

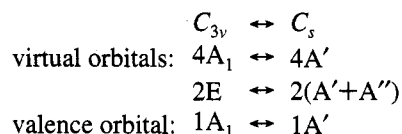
The calculational results presented here are obtained using the HONDO<sup>9</sup> molecular orbital program running on two IBM/risc6000 320H workstations equipped with 64 and 80 MB of memory and 2.6 GB of external disk storage. The coordinate system used to perform the calculations is given in Figure 1. The *x*-axis bisects an ethylene bridge carbon-carbon bond, the negative *z*-axis passes through the nitrogen lone-pair orbital, and the *y*-axis passes between adjacent ethylene bridges. Due to the inherent symmetry of ABCO, the angle labeled  $\Theta$  represents the angle between any two nitrogen-carbon bonds (i.e., the C-N-C angle). A value for this angle is expected to lie between  $109.4^\circ$  for  $\text{sp}^3$  nitrogen atom hybridization and  $120^\circ$  for  $\text{sp}^2$  hybridization. The Dunning-Huzinaga double- $\zeta$  valence (DZV) basis<sup>10</sup> augmented with split 3s functions on the carbon and nitrogen atoms is used (exponents of 0.017 25 and 0.043 70 for carbon and 0.0210 and 0.0532 for nitrogen). An additional calculation also includes split  $3p_{x,y,z}$  orbitals on the nitrogen atom (exponents of 0.018 75 and 0.047 50), in order to check the validity of the qualitative conclusions reached based on the 3s only calculation. The active space chosen for the complete-active-space-self-consistent-field (CASSCF) calculations consists of the doubly occupied nitrogen lone-pair orbital and a set of eight (or 11) virtual orbitals which span the entire 3s (and 3p) Rydberg space representative of the carbon and nitrogen atomic species. The  $3p_{x,y,z}$  nitrogen orbitals are also included in this set for the more complete calculation using the fixed 3s calculation equilibrium geometry. Since HONDO is programmed to utilize only  $D_{2h}$  molecular symmetry and its subgroups, calculations are performed using  $C_s$  symmetry. This

**TABLE 1: *Ab Initio* Calculated State Energies and Structures for ABCO Using the DZV 3s(N and C) Augmented Basis Set**

state symmetry <sup>a</sup>	species energy (hartrees)	relative energy ( $\text{cm}^{-1}$ )	apex angle, <sup>c</sup> $\Theta$ (deg)
Two-Electron CASSCF			
1A'	-326.986 105	0	110.3
2A'	-326.821 792	36 067	114.9
	-326.822 469 <sup>d</sup>		
3A' <sup>b</sup> (1E)	-326.803 205	40 146	114.9
1A'' (1E)	-326.803 191	40 150	114.9
	-326.804 273 <sup>d</sup>		

<sup>a</sup> Equivalent  $C_{3v}$  electron state symmetry given in parentheses. <sup>b</sup> Due to convergence difficulty, a weighted average state was obtained using weights of 1%, 1%, and 98% for the first, second, and third roots, respectively. The energy listed corresponds to the energy of the third root and *not* the state energy. <sup>c</sup> See Figure 1. <sup>d</sup> Obtained with same DZV 3s(N plus C) orbitals as other entries but with  $3p_{x,y,z}(\text{N})$  orbitals added. Calculation performed at the equilibrium geometry calculated for the DZV 3s(N plus C) basis set.

constraint presents no difficulties; the correlation of orbital symmetries between  $C_{3v}$  and  $C_s$  for the active space used is<sup>11</sup>



Excitation within this space (for  $C_s$  symmetry) results in 31 configuration state functions for states of  $A'$  symmetry and 14 configuration state functions for states of  $A''$  symmetry for the 3s active space. For the larger basis set of [3s plus 3p(N)] functions, 51 configuration state functions of  $A'$  symmetry and 27 of  $A''$  symmetry are found. CASSCF wave function convergence difficulties for the 3A' state, which cannot be alleviated using a fully quadratic treatment of the orbital-orbital rotations, are circumvented by calculating a weighted state average. Geometry optimization results are obtained by reducing analytically computed gradients to less than 0.0005 au. Using the above computational system, geometries typically converged after six iterations with a speed of  $\sim 18$  h/iteration.

## III. Results and Discussion

**A. Electronic State Assignment and Spectroscopy.** CASSCF calculational results are presented in Table 1. Listed are geometry-optimized state energies, relative state energies, and the apex angles  $\Theta$ . The electronic state symmetries given in parentheses correspond to equivalent  $C_{3v}$  symmetries. By examining the relative energies listed in the second column, one sees that the third state of  $A'$  symmetry is almost equal in energy to the first state of  $A''$  symmetry, identifying the pair as an E state in  $C_{3v}$  symmetry. Therefore, the calculational results identify the two lowest energy transitions as  $A_1 \leftarrow A_1$  and  $E \leftarrow A_1$ , respectively. Although only fair agreement exists between the two calculated transition energies of 36 067 and 40 150  $\text{cm}^{-1}$ , and the lowest observed transition energies of 39 080 and 43 750  $\text{cm}^{-1}$ , this level of accuracy for transition energies is to be expected from the CASSCF calculational approach.<sup>12</sup> What is in good agreement, as is not atypical, is the energy separation between the excited states:  $\Delta E = 4083 \text{ cm}^{-1}$  calculated, and  $\Delta E = 4670 \text{ cm}^{-1}$  observed. This suggests that the first two (lowest energy) excited states calculated actually correspond to the observed first two transitions.

These calculations support the previous assignment<sup>2</sup> of the first transition as involving a 3s Rydberg excited electronic configuration; however, they suggest that the second observed

**TABLE 2: *Ab Initio* Calculated Natural Orbital Composition for ABCO Ground and First Two Excited Rydberg States (See Figure 1 for Numbering of Atoms)**

CASSCF state and orbital occupancy <sup>a</sup> (e <sup>-</sup> units)	atomic orbital contribution to total wave function (%)											
	atomic orbital atomic(number)	2s N	2p <sub>z</sub> N	3s N	3p <sub>z</sub> N	3s C(2)	3s C(3)	3s C(4)	3s C(5)	3s C(6)	3s C(7)	3s C(8)
1A' (1A <sub>1</sub> ) occ = 1.984		15.1	54.0			1.9	1.0	1.0	1.0	2.5	2.5	2.5
2A' (2A <sub>1</sub> ) <sup>b</sup> occ = 0.987 = 0.990 <sup>c</sup>			6.9	15.8		11.2	16.2	16.2	16.2	5.0	5.0	5.0
			12.4	29.2	2.1	2.0	15.5	15.5	15.5	0.9	0.9	0.9
			9.9	9.4			19.6	19.6	19.6	6.0	6.0	6.0
			12.6	31.5	2.2	1.6	15.2	15.2	15.2	0.3	0.3	0.3
3A' (1E) occ = 1.010 occ = 0.979		1.5	53.3	4.1		1.1	8.2	8.2	13.2			2.2
			0.3			0.3	17.2	17.2	60.4	0.4	0.4	3.6
1A'' (1E) occ = 1.000 = 1.000 <sup>c</sup>		6.1	77.5	5.1								
			35.8	9.4	0.8		12.3	19.6	0.6	4.5	4.7	
							47.2	47.2		2.6	2.6	
			6.3	1.5			31.5	7.9			8.8	8.6

<sup>a</sup> The missing percentages from the CASSCF MOs are from carbon 2p and 2s AOs. <sup>b</sup> These two half-filled orbitals suggest that the 2A<sub>1</sub> configuration arises from a two-electron excitation. <sup>c</sup> Obtained with 3s(N+C) and 3p<sub>x,y,z</sub>(N) basis set.

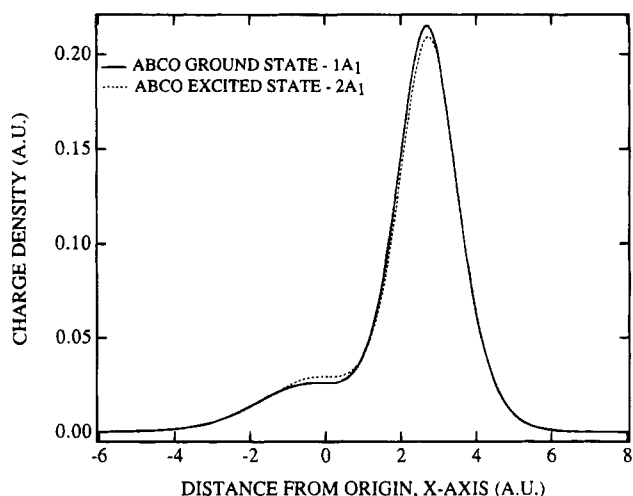


**Figure 2.** Calculated electron charge density along the *x*-axis (see Figure 1) for the 1A<sub>1</sub> and 2A<sub>1</sub> electronic states.

transition also involves a 3s Rydberg excited state. We would thus suggest that the first two electronic transitions of ABCO are 3s Rydberg transitions. Justification for this reassignment is based solely on the high-level CASSCF calculational approach employed in this study and not on estimates of  $\delta$  or analogies with ammonia. The proposed reassignment is additionally supported by calculations employing an expanded DZV + 3s-(N and C) + 3p(N) basis set (see Table 2). This latter set of results demonstrates (see below) that, at the CASSCF level, nitrogen 3p functions do not enter into the description of the first two excited Rydberg states of ABCO to a significant extent. Surely higher excited Rydberg states of a 3p(N and C) nature exist in this system.

Table 1 also presents the apex C-N-C angle  $\Theta$  for each state calculated. Rydberg excitation changes  $\Theta$  from a purely sp<sup>3</sup> hybridization angle of 110.3° to a larger value of 114.9° for each excited state: the nitrogen atom moves inward toward the molecular center of mass upon electronic excitation. This change in nitrogen atom equilibrium position upon Rydberg excitation (2A<sub>1</sub> or 1E) is consistent with the observed activity of the cage compression mode  $\nu_3$  (625 cm<sup>-1</sup>, S<sub>0</sub>) in the 2A<sub>1</sub> ← 1A<sub>1</sub> spectrum.<sup>2,3,6</sup>

Figures 2 and 3 present a plot of the electronic charge density in the 1A<sub>1</sub> ground and 2A<sub>1</sub> first excited states of ABCO. Figure

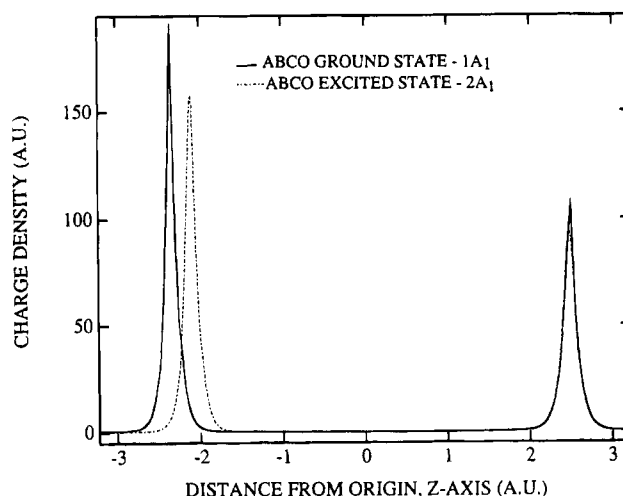


**Figure 3.** Calculated electron charge density along the *z*-axis (see Figure 1) for the 1A<sub>1</sub> and 2A<sub>1</sub> electronic states.

2 shows the calculated charge density along the *x*-axis (see Figure 1). Note that (1) the charge density between the ethylene bridges (*-x*-axis) is much less than that between an ethylene C-C bond (*+x*-axis) and (2) the overall *x*-axis charge density changes little between the two electronic states mapped. Figure 3 shows the same calculation for the *z*-axis. Note in this instance that (1) the charge density is highest for the N atom (*-z*-axis) and (2) the electron charge density at the N atom is greatly altered (toward the molecular center of mass) in position and value along the *z*-axis upon Rydberg state excitation. This position change is consistent with the result that the apex angle  $\Theta$  increases from 110.3° to 114.9° in the electronic excitation. The 10% decrease in *z*-axis integrated (total) charge density for the excited state is expected in a local 2p<sub>z</sub> to diffuse 3s electronic promotion. The overall change in charge density from S<sub>0</sub> to S<sub>1</sub> is not inconsistent with the qualitative notion that the electron distribution should be more diffuse in the Rydberg state than in the ground state. Two effects can be characterized upon S<sub>1</sub> ← S<sub>0</sub> excitation: electron density is removed from a localized *z*-axis directed orbital to more diffuse "spherical" orbitals on both N and C atoms; and the molecular geometry changes. Thus, although the maximum in the charge density along the *z*-axis moves closer to the origin for the Rydberg states, the charge density is more diffuse along the other two orthogonal directions.

**B. Natural Orbital Interpretation of Electronic State Composition.** To gain insight into the electronic state orbital structure for each of the states calculated, a summary of natural orbital composition is presented in Table 2. The columns of Table 2 list the percentage contribution of the various atomic orbitals which constitute a given "active space" molecular orbital (MO). The ground electronic state CASSCF result for the highest occupied MO, listed in the first row, is an MO composed mainly of  $2p_z$  and  $2s$  atomic orbitals (AO), with many residual AOs contributing to the total MO. This orbital is doubly occupied (first column) and corresponds to the nitrogen lone-pair orbital. The second and fourth rows of Table 2 correspond to the electronically excited  $2A_1$  state. Here, both of the partially occupied highest orbitals have an occupancy of roughly one electron. Both of these orbitals are similar in that neither contains significant  $2s$  or  $2p_z$  character; this is a somewhat surprising result since conceptually one is tempted to envision the excited state as comprising a  $2p_z$  nitrogen orbital on nitrogen containing one electron and a  $3s$  nitrogen Rydberg orbital containing a second electron. Given the orbital composition of this excited  $A_1$  state, the  $2A_1 \leftarrow 1A_1$  transition may probably best be thought of as a two-electron excitation (see Table 2). Additionally, the Rydberg orbital delocalization over the molecule can be assessed for Table 2; the  $2A'$  state is roughly equally composed of  $3s$  AOs from atoms N(1) and C(3,4,5) (ca. 15–20%) and to a less extent  $3s$  atomic orbitals from C(6,7,8). The natural orbital compositions for the  $3A'$  and  $1A''$  (E) states are also listed in Table 2: the results for these states are not as clear-cut as those for the first excited Rydberg state. The  $3s$  active space basis set compositions suggest a delocalized E Rydberg state composed of  $3s$  AOs from carbon atoms 3, 4, and 5 and an overall one-electron transition for the excitation  $1E \leftarrow 1A_1$ . The extended [ $3s$  plus  $3p(N)$ ] basis set yields natural orbitals that are also delocalized over the carbon  $3s$  orbitals but suggests that the  $2p(N)$  orbital has reduced electron density. One must be cautious here because the  $1E$  state is high in energy and could still change with further basis set expansion.

Two important conclusions regarding experimental data can be obtained from these Rydberg orbital delocalization results. First, the calculated  $2A_1$  excited state delocalization over only atoms 1, 3, 4, and 5 is consistent with experimental ABCO/argon studies for the  ${}^1R_1$  ( $2A_1$ ) state.<sup>7</sup> The experimentally observed cluster conformation with the argon atom located near the nitrogen atom of ABCO exhibits spectral broadening, electron transfer, and an increased intersystem crossing rate, whereas the cluster conformation with the argon atom located near the tertiary carbon of ABCO does not exhibit any of these

phenomena. Second, the calculated delocalization is consistent with reassignment of the second observed transition and inconsistent with the previous assignment based on the concept of a localized (nitrogen atom) transition.

#### IV. Conclusions

We present a CASSCF study of the ground and first two excited (Rydberg) states of ABCO. The results support the reassignment of the second excited state as a  $3s$  Rydberg state. The first two excited states ( $2A'$  and  $1E$ ) are composed of  $3s$  atomic orbitals from both carbon and nitrogen atoms. The computed change in ABCO structure upon Rydberg state excitation (i.e.,  $\Delta\Theta(C-N-C) \sim +4^\circ$ ) due to the change in hybridization of the nitrogen atomic center is consistent with the identification of the cage compression mode as the progressing forming mode in the  $2A_1 \leftarrow 1A_1$  electronic transition. The calculations point to the importance of both carbon and nitrogen  $3s/3p$  orbitals for the excited state molecular orbital composition. Additionally, the first excited state appears to be best classified as a two-electron excitation from the ground state.

**Acknowledgment.** This effort is supported by the National Science Foundation and the U.S. Army Research Office. We thank Professor A. K. Rappé for many helpful discussions and suggestions during the course of the work.

#### References and Notes

- (1) Robin, M. B. *Higher Excited States of Polyatomic Molecules*; Academic Press: New York, 1974; Vol. 1.
- (2) Parker, D. H.; Avouris, P. *Chem. Phys. Lett.* **1978**, *53*, 515.
- (3) Halpern, A. M.; Roebber, J. L.; Weiss, K. *J. Chem. Phys.* **1968**, *49*, 1348.
- (4) Halpern, A. M. *Chem. Phys. Lett.* **1970**, *6*, 296.
- (5) Douglas, A. E.; Hollas, J. M. *Can. J. Phys.* **1969**, *39*, 479.
- (6) Gonohe, N.; Yatsuda, N.; Mikami, N.; Ito, M. *Bull. Chem. Soc. Jpn.* **1982**, *55*, 2796.
- (7) (a) Shang, Q. Y.; Moreno, P. O.; Li, S.; Bernstein, E. R. *J. Chem. Phys.* **1993**, *98*, 1876. (b) Shang, Q. Y.; Moreno, P. O.; Bernstein, E. R. *J. Am. Chem. Soc.* **1994**, *116*, 302, 311.
- (8) Avouris, P.; Rossi, A. R. *J. Phys. Chem.* **1981**, *85*, 2340.
- (9) Dupuis, M.; Marquez, A. *HONDO 8.4*; IBM Corporation, Department MLM/428: Kingston, NY, 1992.
- (10) Dunning, T. H.; Hay, P. J. In *Methods of Electronic Structure Theory*; Schafer, H. F., III, Ed.; Plenum Press: New York, 1977; p 1.
- (11) Wilson, E. B., Jr.; Decius, J. C.; Cross, P. C. *Molecular Vibrations—The Theory of Infrared and Raman Vibrational Spectra*; Dover Pub. Co.: New York, 1955.
- (12) See for example: (a) Disselkamp, R.; Im, H. S.; Bernstein, E. R. *J. Chem. Phys.* **1992**, *97*, 7889. (b) Disselkamp, R.; Bernstein, E. R.; Seeman, J. I.; Secor, H. V. *J. Chem. Phys.* **1992**, *97*, 8130.

JP941046F